

Single-cell transcriptome landscape elucidates the cellular and developmental responses to tomato chlorosis virus infection in tomato leaf

Hao Yue^{1,2}  | Gong Chen³ | Zhuo Zhang¹ | Zhaojiang Guo⁴ |
 Zhanhong Zhang⁵ | Songbai Zhang¹ | Ted C. J. Turlings⁶  | Xuguo Zhou⁷ |
 Jing Peng¹ | Yang Gao¹ | Deyong Zhang^{1,2} | Xiaobin Shi^{1,2} | Yong Liu^{1,2}

¹Institute of Plant Protection, Hunan Academy of Agricultural Sciences, Changsha, China

²Longping Branch, College of Biology, Hunan University, Changsha, China

³College of Plant Protection, Hunan Agricultural University, Changsha, China

⁴Institute of Vegetables and Flowers, Chinese Academy of Agricultural Sciences, Beijing, China

⁵Institute of Vegetable, Hunan Academy of Agricultural Sciences, Changsha, China

⁶Laboratory of Fundamental and Applied Research in Chemical Ecology, Institute of Biology, University of Neuchâtel, Neuchâtel, Switzerland

⁷Department of Entomology, University of Kentucky, Lexington, Kentucky, USA

Correspondence

Yong Liu, Xiaobin Shi and Deyong Zhang,
 Institute of Plant Protection, Hunan Academy of Agricultural Sciences, Changsha, China.
 Email: haoasliu@163.com, shixiaobin@hunaas.cn and dyzhang78@163.com

Funding information

National Natural Science Foundation of Hunan Province, Grant/Award Number: 2023JJ10026; National Natural Science Foundation of China, Grant/Award Numbers: 32030088, 32072383, 32272535, 31901854; Agriculture Research System of China, Grant/Award Number: CARS-23-D-02

Abstract

Plant viral diseases compromise the growth and yield of the crop globally, and they tend to be more serious under extreme temperatures and drought climate changes. Currently, regulatory dynamics during plant development and in response to virus infection at the plant cell level remain largely unknown. In this study, single-cell RNA sequencing on 23 226 individual cells from healthy and tomato chlorosis virus-infected leaves was established. The specific expression and epigenetic landscape of each cell type during the viral infection stage were depicted. Notably, the mesophyll cells showed a rapid function transition in virus-infected leaves, which is consistent with the pathological changes such as thinner leaves and decreased chloroplast lamella in virus-infected samples. Interestingly, the F-box protein SKIP2 was identified to play a pivotal role in chlorophyll maintenance during virus infection in tomato plants. Knockout of the *SISkip2* showed a greener leaf state before and after virus infection. Moreover, we further demonstrated that *SISkip2* was located in the cytomembrane and nucleus and directly regulated by ERF4. In conclusion, with detailed insights into the plant responses to viral infections at the cellular level, our study provides a genetic framework and gene reference in plant-virus interaction and breeding in the future research.

KEY WORDS

cell atlas, single-cell RNA sequencing (scRNA-seq), *Solanum lycopersicum*, ToCV infection, transcriptional factor

1 | INTRODUCTION

Plant viral diseases contribute significantly to crop yield loss and threaten crop production worldwide, and tend to be more serious under extreme temperatures and drought climate changes. With global warming, plant viruses are estimated to cause losses exceeding 50 billion euros per year (Pallás et al., 2018), and with the increasing

human population and food requirements, reducing the impact of viruses on crop yields will remain a challenge of top priority (Gessain and García-Arenal, 2015). The tomato chlorosis virus (ToCV, genus Crinivirus, family Closteroviridae) was first discovered in Florida in 1998 and has since spread to 35 countries and regions (Wisler et al., 1998a; 1998b; Yang et al., 2020). ToCV infects tomato plants at a high frequency (50%–100%) and can reduce tomato yield by more

than 50% (Fortes and Navas-Castillo, 2012; Lozano et al., 2006; Velasco et al., 2008). To date, there is no effective way to control ToCV transmission (Lozano et al., 2006), and the molecular mechanism of ToCV infection is unclear (Shi et al., 2021). A transcriptional map at cellular resolution may help unravel the process of ToCV infection and help understand how such virus infection represses plant immunity and alters plant development.

Cells play distinct biological roles in plant development and environmental adaptation. Mapping and quantifying transcriptional activity at single-cell resolution can provide insights into the molecular networks associated with cell-specific physiological and developmental processes (Libault et al., 2017). Since 2019, single-cell technology has been used to explore developmental trajectories and transcriptional regulation pathways in plants at high spatial resolution (Efroni and Birnbaum, 2016; Shaw et al., 2021). For example, it has been demonstrated that *Arabidopsis* cells are showed to be transcriptomically highly heterogeneous, and the construction of single-cell transcriptional profiles of *Arabidopsis* tissue lays a good foundation for analyzing the molecular mechanisms of *Arabidopsis* development and identifying regulatory genes (Denyer et al., 2019; Jean-Baptiste et al., 2019; Zhang et al., 2019; Zhang et al., 2021). Moreover, similarities and divergence between the shoot and root apex of *Arabidopsis* at single-cell resolution have been identified (Liu et al., 2021a; Zhang et al., 2021). Single-cell studies have also been conducted in "non-model" plants such as maize and peanuts. For example, the molecular mechanism by which the SHORT-ROOT pathway regulates the complexity of cortex tissue in maize roots has been examined in detail (Ortiz-Ramírez et al., 2021). Leaves are necessary for plants' photosynthesis, growth, and development (Du et al., 2018). Recently, single-cell RNA sequencing (scRNA-seq) has been used to describe the transcriptome landscape and identify critical transcription factors (TFs) in the leaf blades of allotetraploid peanuts (Liu et al., 2021b). However, no studies have been reported to elucidate the molecular mechanisms of tomato leaf response to biotic and abiotic stresses at the cellular level.

As sessile organisms, plants require significant flexibility in their transcriptional response programs to environmental exposure and daily challenges (Shaw et al., 2021). The primary cellular activities involved in plant development and stress adaptation, such as the response to abiotic stress at the cellular level, have been investigated using scRNA-seq (Rich-Griffin et al., 2020). The heat stress on *Arabidopsis* seedlings results in the dominant expression of heat shock genes across cell types, with subtle differences detected in other genes (Jean-Baptiste et al., 2019). Treatment of *Arabidopsis* roots with sucrose alters the proportion of cells from each cell type cluster. The hair cells from plants treated with sucrose are highly enriched (Shulse et al., 2019). High-salinity treatment uniformly reduced the proportion of mesophyll cells and the abundance of chlorophyll-binding proteins in each mesophyll cell (Liang et al., 2023; Wang et al., 2021). The cellular and molecular characteristics of woodland strawberry leaves at different disease stages were identified using scRNA-seq (Bai et al., 2022). To date, no study has

used the single-cell approach to study plant responses to biotic stresses, such as virus infection.

In this study, we applied single-cell sequencing on ToCV-infected tomato leaves and aimed to elucidate the molecular mechanisms of plant response to the virus at the cellular level. Based on the expression patterns for cell lineage responses to ToCV infection, we characterized potential pathways and genes associated with disease resistance. Changes in the number of mesophyll cells and in the internal structure of leaves were shown to be directly related to the phenotype resulting from ToCV infection. Notably, the *SISKP2* was identified as a positive role in chlorophyll maintenance during ToCV infection in tomato plants for the first time, and we demonstrated that it was regulated by ethylene-responsive element binding factor 4 (ERF4). The study confirms the potential of the single-cell transcriptomics approach for research on plant–virus interactions and provides new insights into the regulatory mechanisms in plant research and breeding to control plant viruses.

2 | MATERIALS AND METHODS

2.1 | Plant materials and growth conditions

Tomato plants (*S. lycopersicum* Mill. cv. 'Zuanhongmeina') were used for all the experiments. The plants were kept in an insect-proof cage in a greenhouse under a light/dark photoperiod of 16/8 h at 26°C. ToCV-infected plants were obtained as previously described (Yue et al., 2021). In brief, a ToCV infectious cDNA agro clone was injected into three-true-leaf-stage tomato plants. Visual (leaf chlorosis) and molecular (real-time quantitative PCR [RT-qPCR]) analyses were conducted to confirm the viral infection. The sequence information for the ToCV-specific RT-qPCR primers is listed in Table S1.

2.2 | Preparation of single-cell suspensions and a single-cell RNA-seq library

Protoplasts were isolated from the leaves of healthy noninfected plants (H) and plants infected with ToCV (V). The initial and rapid periods of virus growth were selected as case samples. The leaves of the tomato plants were removed and immediately transferred into enzyme solution (10 mM CaCl₂, 20 mM KCl, 20 mM MES, 2% Cellulase R-10, 1% Pectolyase Y-23, 0.1% BSA, 0.4% macerozyme R-10, 0.4 M mannitol, pH 5.7) by vacuum infiltration for 30 min. The samples were then protoplasted for 2 h at 20°C on an orbital shaker set at 200 × g. Cells were filtered with a 40 µm cell strainer. WI solution (4 mM MES, 4 mM KCl, 0.3 mM mannitol at pH 5.7) was added and shaken vigorously to release the protoplasts. The samples were washed with the WI solution; the protoplasts in the supernatant were collected by centrifugation at 200 × g. Cell activity was detected by trypan blue staining, and cell concentration was measured using a hemocytometer. The scRNA-seq libraries were constructed using the Chromium Single Cell 3' Gel Beads-in-emulsion (GEM) Library & Gel Bead Kit v3.

2.3 | Single-cell RNA-seq data preprocessing

The 10x Genomics official software Cell Ranger (version 3.1.0) was used to perform quality statistics on the raw data and map the reads to the *S. lycopersicum* reference genome (Butler et al., 2018). The transcripts were quantified using the STAR aligner. The software uses barcode sequence markers in the identification sequence to distinguish cells and the UMI markers of different mRNA molecules in each cell to transcribe high-throughput single cells. Quantification was performed, and quality control statistics such as high-quality cell number, gene median value, and sequencing saturation were obtained. The Seurat software package (version 3.0) was used to perform further quality control and process the data based on the preliminary quality control results of Cell Ranger (Butler et al., 2018). In theory, the number of genes expressed by the cells, the number of UMIs, and the quantity of mitochondrial gene expression are concentrated in a specific area. Therefore, cells with gene numbers and UMI numbers within \pm two standard deviations of the mean and with a ratio of mitochondrial genes of less than 0% were retained as high-quality cells for downstream analysis. Library size normalization was performed in Seurat on the filtered matrix to obtain the normalized count.

2.4 | Cell clustering and identification of marker genes

The top variable genes across single cells were identified using a previously described method (Macosko et al., 2015). Briefly, the average expression and dispersion were calculated for each gene, and the genes were subsequently placed into several bins based on their expression. Mutual nearest neighbours were used to reduce the dimensionality of the log-transformed gene-barcode matrices of the top variable genes. The cells were clustered using a graph-based clustering approach and visualized in two-dimension using tSNE. A likelihood ratio test that simultaneously tests for changes in mean expression and percentage of expressed cells was used to identify the marker genes of a cluster. Multimodal intersection analysis (MIA) (Moncada et al., 2020), a novel computational method for unbiased cell type recognition of scRNA-seq, was used to infer the origin of every single cell independently and to identify cell types.

2.5 | Functional analysis

Differentially expressed genes (DEGs) were identified using the Seurat package (Butler et al., 2018). A p -value < 0.05 and $|log2foldchange| > 1$ (or $|log2foldchange| > 0.58$) was set as the threshold for significantly differential expression. GO enrichment and Kyoto Encyclopedia of Genes and Genomes (KEGG) pathway enrichment analyses of DEGs were performed using R based on the hypergeometric distribution. The intersection size of DEGs across cell types was visualized using the function 'upset' in the UpSetR R package (version 1.4.0) (Lex et al., 2014).

2.6 | RNA in situ hybridization

RNA in situ hybridization was performed as previously described (Zhang et al., 2017). In brief, tomato leaves were fixed with formaldehyde and embedded using a tissue spreader (Kedi, KD-P). Paraffin-embedded samples were sectioned (7–9 mm) using a pathology slicer (Leica RM2016). The slides were dewaxed, digested with proteinase K (Servicebio, G1205), dehydrated with a gradient of ethanol, and hybridized with probes. After washing, the slides were incubated with anti-DIG-AP (Jackson, 200-052-156) and washed in TBS four times for 5 min each. Signals were detected using NBT/BCIP stock solution (Boster). Images were obtained using a Nikon DS-U3 microscope (Nikon). The primers used are listed in Table S1.

2.7 | Anatomical study

The slices were placed in xylene I for 20 min, xylene II for 20 min, anhydrous ethanol I for 5 min, anhydrous ethanol II for 5 min and 75% ethanol for 5 min, then washed with water. Next, the plant tissue slices were placed in the dye solution for approximately 2–5 min, washed with water, and examined under a microscope. Differentiation and non-differentiation were performed according to the degree of tissue staining. After washing, slices were placed in an oven and dried. The slices were placed into clean xylene transparent for 5 min. The slide was mounted with neutral gum and observed using an optical microscope. The leaf thickness and the proportion of leaf cells were measured from the acquired images using ImageJ software.

2.8 | Transmission electron microscopy

Tomato leaves were cut into pieces and fixed overnight at 4°C in fixation buffer (2.5% glutaraldehyde, 0.05 M phosphate, pH 7.2). Samples were then washed three times with fixation buffer followed by postfixation in 2% osmium tetroxide at 4°C for 2 h. After dehydration in a graded ethanol series (50%, 70%, 80%, 90%, 95%, and 100%), the tissue samples were embedded in Spurr's resin. Ultrathin sections (70–90 nm) were cut using a Leica EM UC7 ultramicrotome and sequentially stained with uranyl acetate for 20 min and Reynolds' lead citrate for 5 min. The sections were then viewed with a JEM-1230 transmission electron microscope operated at 80 kV.

2.9 | Gene set variation analysis (GSVA)

GSVA converts the gene expression matrix of different samples/cell populations into the gene expression matrix among them to evaluate whether different metabolic pathways are enriched in different samples/cell populations (Zhong et al., 2022). The rank statistics calculation, similar to the KS test, was performed for the gene set

corresponding to each pathway, and the expression matrix was converted into a pathway enrichment score matrix; the GSVA enrichment score was obtained for each cell corresponding to each pathway. Pathways with significant differences were obtained by limma packer analysis, allowing the degree of enrichment for different pathways in different groups to be evaluated (Ritchie et al., 2015).

2.10 | Pseudo-time trajectory analysis and regulatory network

Pseudo-time trajectory analysis of the single-cell transcriptome was conducted using Monocle 2 (Trapnell et al., 2014). Machine learning was performed based on key gene expression patterns to simulate the developmental process's dynamic changes over time. The genes with a significant degree of gene expression variation between cells were selected, spatial dimensionality reduction was performed based on their expression profiles, and then a minimum spanning tree (MST) was constructed. The longest path was found through the MST to represent similar transcription characteristics to the cell's different trajectory. TFs and their target genes were obtained from <http://plantregmap.gao-lab.org/download.php>. The interaction relationship table of TF differential target genes was obtained according to the name matching the differential genes, and the network diagram was visualized using Cytoscape.

2.11 | Construction and transformation of transgenic tomato

The CRISPR/Cas9 plant expression vector (pYLCRISPRCas9Pubi-H) and sgRNA expression vector (pYLgRNA) were constructed as previously described (Ma et al., 2015). The binary constructs were transformed into *Agrobacterium tumefaciens* strain EHA105 via electroporation. The *A. tumefaciens* cells containing the recombinant plasmid were introduced into tomato (*S. lycopersicum* Mill. Cv. MicroTom). Transgenic plants were obtained after cocultivation and screening. Homozygous transgenic plants were used in all experiments. The designed guide RNA (gRNA) sequences and detection primers are listed in Table S1.

2.12 | Yeast-one-hybrid assays and dual-LUC assay

The promoter sequences from *SISkip2* were cloned into the pAbAi vector, and the full-length *ERF4* cDNA was cloned into the pGADT7 vector. The pAbAi-baits were transformed into the Y1HGold yeast genome and screened on selective drop out (SD)-Ura medium with different aureobasidin A (AbA) concentrations. The AD-prey vectors were transformed into the bait strain and screened on an SD/-Leu/AbA plate. For the dual-LUC assay, the coding sequence of *ERF4* and the region upstream of the start codon of *SISkip2* were introduced

into the effector (pGreenII 62-SK) and reporter (pGreenII 0800-LUC) vectors, respectively. The recombinant vectors were transformed into *A. tumefaciens* strain GV3101, and the bacterial mixture carrying different vectors was co-infiltrated into *Nicotiana benthamiana* leaves. After 72 h, leaf discs were collected for the measurement of relative LUC activities with the Dual-LUC Reporter Assay System (Promega) using a Glomax 2020 Single Tube Luminometer instrument (Promega). Empty pGreenII 62-SK and pGreenII 0800-LUC vectors were used as negative controls. The primers used are listed in Table S1.

2.13 | Subcellular localization

The full-length coding sequences of *SISkip2* were inserted into the BamH I and Xba I sites of pFGC-eGFP vector to generate the *SISkip2*-eGFP fusion genes driven by a CaMV35S promoter (Chen et al., 2018). *Agrobacterium tumefaciens* cultures containing the *SISkip2*-eGFP and pFGC-eGFP construct were independently infiltrated into 4-week-old *N. benthamiana* leaves expressing the red nuclear marker RFP-H2b (Chen et al., 2018). After 48 h of incubation, fluorescent signals were observed under a Nikon confocal laser scanning microscope (A1-SHS; Nikon).

3 | RESULTS

3.1 | Generation of a single-cell transcriptome atlas of tomato leaf cells

scRNA-seq was performed using the 10 \times Genomics platform and Illumina sequencing (Figure 1a). Data were pre-filtered at the cell and gene levels, and 13 720 cells with 938 genes/cell, 9506 cells with 1473 genes/cell for samples H (healthy 'noninfected', control) and V (plants infected with ToCV) were successfully profiled (Figure S1a). Graph-based unsupervised clustering and differential expression analysis provided insights into the tomato leaf tissues. The cells were divided into eight clusters, with the percentage of cells in each cluster ranging from 4% to 18% (Figure S1b,c). After annotation, all cell clusters were categorized into six cluster clouds corresponding to trichome cells, mesophyll cells, proliferating cells, guard cells, vascular cells and epidermal cells (Figure 1c).

The mesophyll cell population consisted of two clusters (clusters 2 and 5), in which genes involved in photosynthesis, including chlorophyll A-B binding protein 1b (CAB1b), photosynthetic NDH subunit of subcomplex B4 (PNSB4) and ribulose bisphosphate carboxylase small chain 3b (RBCS3b), were predominantly expressed (Figure 1d) (Endo et al., 2014; Kim et al., 2021; Sawchuk et al., 2008; Zhang et al., 2021). Clusters 2 and 5 showed an abundance of marker genes implicated in processes related to photosynthesis and response to light stimulus (Figure 1d; Table S2). Guard cells were found in clusters 4 and 7 because genes homologous to *Arabidopsis* guard cell-

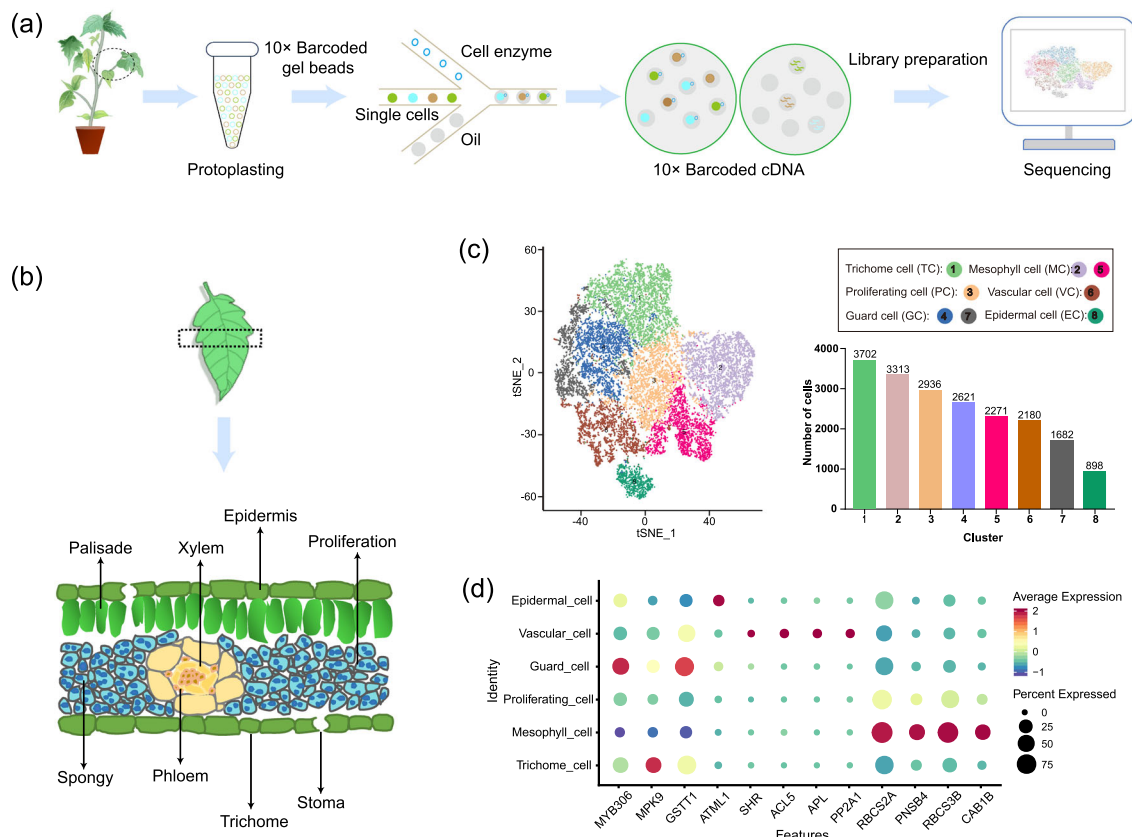


FIGURE 1 Single-cell RNA-seq and cluster annotation of tomato leaf. (a) Brief process of isolation of tomato leaf protoplast cells and scRNA-seq. (b) Schematic of anatomy and cell types of tomato leaf. (c) Visualization of six broad populations using t-SNE and number of cells in each cluster. (d) Expression of cell-type marker genes for each cluster. Dot diameter, proportion of cluster cells expressing a given gene; colour, mean expression across cells in that cluster.

specific genes MAP kinase and MYB60 were enriched in these clusters (Figure 1d). The vascular cells were assigned to cluster 6, in which the following genes were expressed: the phloem-related genes altered phloem development (APL) and phloem protein 2a1 (PP2a1) (Bonke et al., 2003; Ruonala et al., 2017); and the xylem-related genes ACAULIS 5 (ACL5) and SHORT ROOT (SHR) (Figure 1d) (Sun et al., 2022; Wendrich et al., 2020). Cluster 8 comprised epidermal cells in which genes homologous to *Arabidopsis* epidermal-specific genes were enriched, such as MERISTEM LAYER 1 (ATML1) and Glutathione S-Transferase T1 (GSTT1) (Figure 1d) (Javelle et al., 2011; Liu et al., 2021b; Takada et al., 2013). In addition, MIA was used to assist in identifying remaining clusters (Moncada et al., 2020). The gene sets were defined by identifying for each cell type those genes whose expression is statistically higher in the cells annotated to that cell type in comparison with expression in the remaining cells (Table S3). The results showed that cluster 1 represented trichome cells, and cluster 3 represented proliferating cells (Figure S2). Altogether, the results indicate that the tomato leaf is composed of highly heterogeneous cells (Figure 1d), verifying the reliability of the experimental and computational procedures for single-cell transcriptome analyses.

3.2 | Identification and functional characterization of potential marker genes

To characterize the specific marker genes of the tomato leaf cell types, sample H was isolated to exclude the influence of ToCV infection. The difference in expression between the specified cell population and all other cell populations was tested, and each cell population's potential specific marker genes were identified. The top 10 genes with the highest expression levels in each cluster were collected, and their expression profiles were described in a heatmap (Figure 2a; Figure S3). The eight representative genes with the highest expression in each cell type were selected for display on the t-SNE map (Figure 2b). The results of the RNA in situ hybridization assays were consistent with the cell types identified (Figure 2c-e). Thus, solyc11g022590.1, solyc02g082920.4, and solyc06g061230.3 were proved as marker genes for tomato leaf mesophyll, guard, and phloem cells, respectively. GO analyses revealed that cluster-specific marker genes were involved in diverse biological processes such as response to wounding and response to light stimulus (Figure 2f; Table S4). Based on the KEGG annotations, the enriched pathways were primarily involved in photosynthesis-antenna protein synthesis

and protein processing in the endoplasmic reticulum (Figure S4 and Table S5). The characterization of potential marker genes of different cell types in tomato leaves can be used for further research on tomato plants using single-cell technology and provides an essential reference for other plants.

3.3 | Single-cell heterogeneity analysis of tomato leaf infected by ToCV

We first characterized the single-cell expression profiles of tomato leaves infected by ToCV to reveal cell-to-cell heterogeneity of

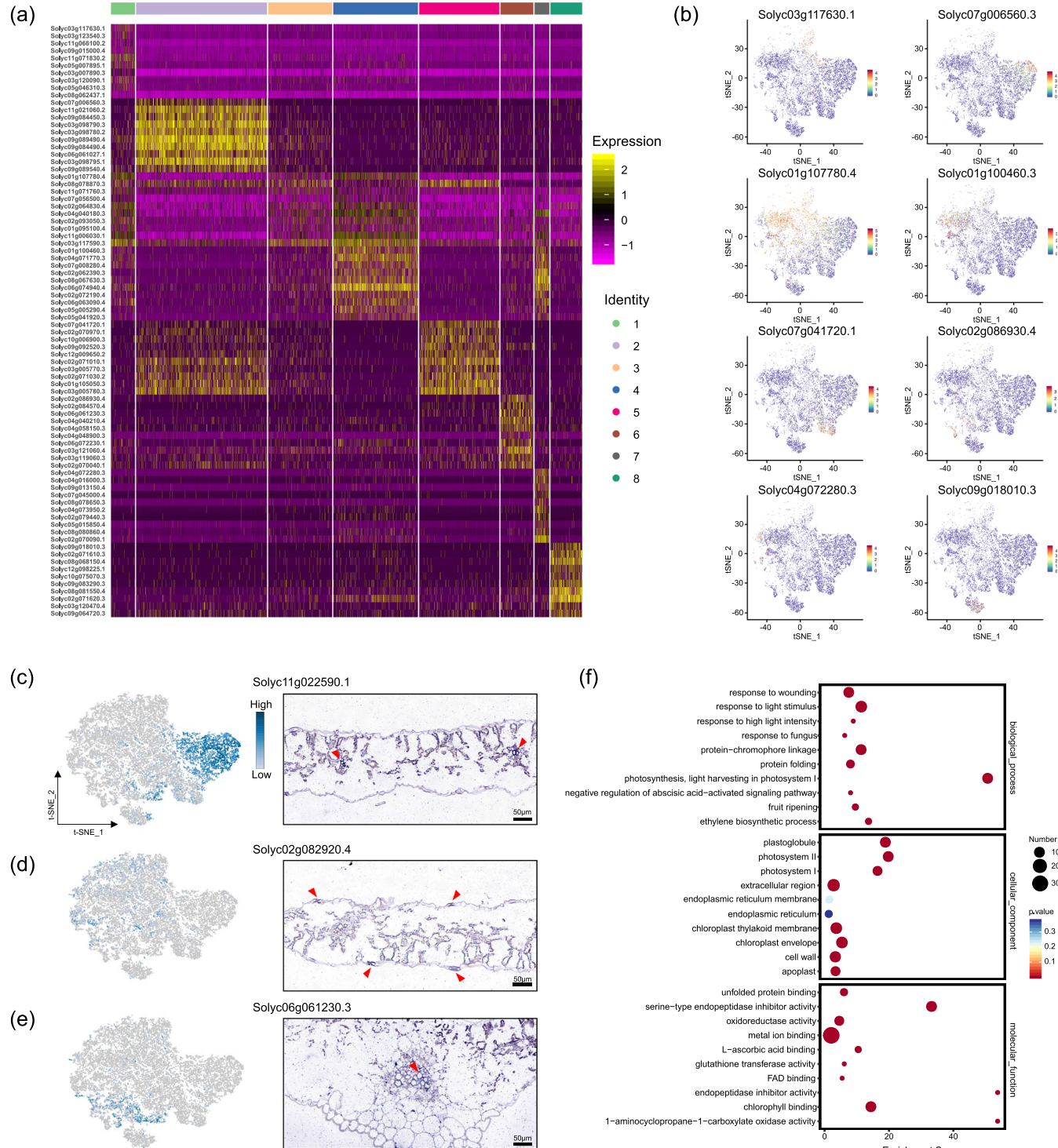


FIGURE 2 Identification of new marker genes within cell-type clusters. (a) Heatmap shows each cluster's top ten DEGs with the highest expression levels. (b) Expression patterns of eight new marker genes distributed in a t-SNE map. (c–e) t-SNE visualization and RNA in situ hybridization assays for three clusters-specific genes in the tomato leaf. Scale bars, 50 μm. (f) GO enrichment analysis of all marker genes. DEGs, differentially expressed genes. [Color figure can be viewed at wileyonlinelibrary.com]

tomato leaf response to ToCV (Figure 3a). Notably, the analysis of cell proportions between the two subgroups of the control (H) and treatment (V) showed that the tomato leaf responded markedly to the ToCV stimulus. It can be clearly observed that there was a significant increase in the proportion of trichome cells (increased

from 5.1% to 38.9%), while the proportion of mesophyll cells and epidermal cells were significantly reduced (decreased from 45.6% to 3.4% and 6.8% to 1.2%, respectively) (Figure 3b). The UMI reflects the number of transcripts captured by scRNA-seq. Different cell clusters exhibited distinct transcriptional characteristics after ToCV

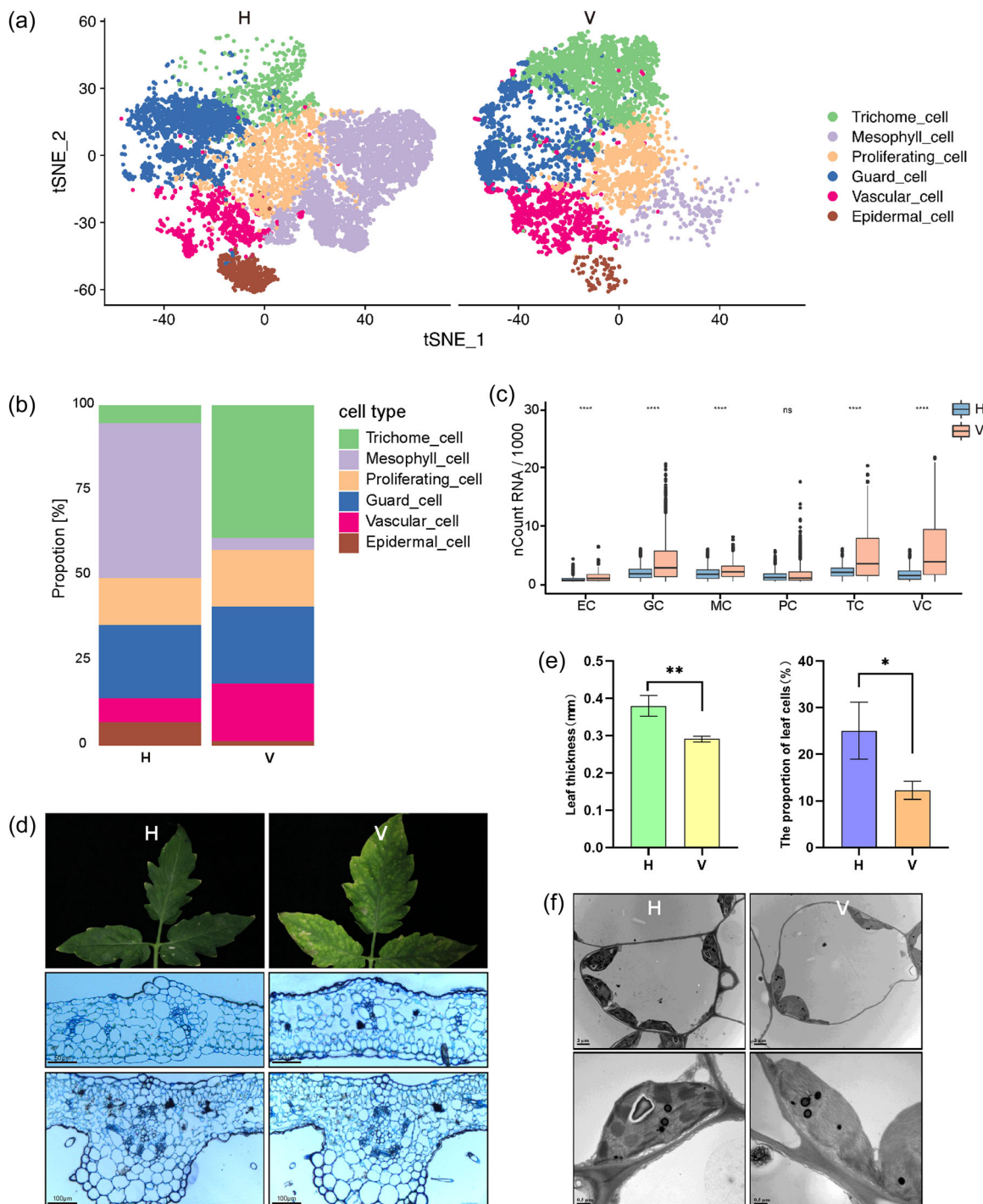


FIGURE 3 Changes of cell-type frequencies and gene expression after tomato chlorosis virus (ToCV) infection. (a, b) Visualization of clusters distribution of control and case samples. (c) Total UMI values for each cell type in control and ToCV-infected leaf samples. (d) Healthy and ToCV-infected tomato plants and toluidine blue staining of healthy and ToCV-infected tomato leaves. (e) Quantification of leaf thickness and the proportion of leaf cells. (f) Electron microscopic observation of healthy and ToCV-infected tomato leaves. Values are means \pm SE. Asterisks denote significant differences ($p < 0.05$). Six replications were used for each measurement. [Color figure can be viewed at wileyonlinelibrary.com]

infection (Figure 3c). Directly related to this strong response are the internal morphological structure and phenotype of tomato leaves. For example, ToCV-infected leaves exhibit severe symptoms of interveinal yellowing (Figure 3d). The morphological features of healthy and ToCV-infected tomato leaves were observed using an optical microscope. Compared to healthy tomato leaves, the ToCV-infected leaves were thinner, and the internal cell arrangement was loose (Figure 3e). In addition, electron microscopy results showed that the pathological changes in virus-infested samples were mainly in phloem and mesophyll cells, and the number of chloroplast lamella decreased (Figure 3f). To explore the level of heterogeneity, the regulation of DEGs after ToCV infection was analyzed (Figure S5a). Results showed that some DEGs were shared between different cell types, but the DEGs were mainly represented in a single cell type (Figure S5b).

3.4 | Characterization of expression profiles for cell lineage response to ToCV infection

To gain insight into expression patterns of cell genes responding to ToCV infection, GO and KEGG pathway analysis were further performed on these significantly expressed DEGs. The results of differential gene expression enrichment analysis revealed tomato leaves' transcriptional response to ToCV infection, with certain commonalities among the cell types (Table S6). Not surprisingly, the defence-related pathways were significantly enriched and upregulated in six cell subsets, such as mitogen-activated protein kinases (MAPK) signalling pathway and plant-pathogen interaction (Figure S6). Consistently, among the upregulated DEGs, for example, the GO terms 'defence response' and 'response to chitin' were enriched significantly and shared in most ToCV-infected cell types (Figure 4a). Moreover, in epidermal cells, mesophyll cells and proliferating cells, the upregulated DEGs showed signatures for

'chlorophyll metabolic process' and 'malate transmembrane transport (Figure 4a)'. Interestingly, the upregulated genes in vascular cells and guard cells were mainly enriched in GO term 'tyrosine biosynthetic processes'. In trichome cells, 'oxidation-reduction process' and 'response to molecule of bacterial origin' were significantly enriched (Figure 4a).

Next, gene set variation analyses (GSVA) with all DEGs were performed to investigate the molecular mechanisms and pathways involved in the differential responses to ToCV infection among cell types. Following ToCV infection, the synthesis and metabolism of several secondary metabolites were significantly induced in different cell types, such as steroid biosynthesis in mesophyll cells, proliferating cells and trichome cells; phenylpropanoid biosynthesis in epidermal cells; and brassinosteroid (BR) biosynthesis in vascular cells (Figure S7). The absorption and utilization of light energy in plants are directly affected by light-harvesting antenna proteins (Sun et al., 2021), and a similar result was found in our research that the highly expressed gene sets in the proliferating cells were involved in the synthesis of photosynthesis-antenna proteins (Figure S7).

3.5 | Differentiation trajectory of mesophyll cells affected by ToCV infection

To reveal the developmental trajectories of tomato cell types during ToCV infection and key regulatory genes during differentiation, Monocle 2 was used to apply pseudo-time analysis to the clusters of specific cell types in tomato leaves (Trapnell et al., 2014). We focused on mesophyll cells as they are in close association with the plant phenotype resulting from ToCV infection. The gene expression matrices of mesophyll cells generated from samples H and V were used to construct the differentiation trajectory (Figure 5a). The pseudo-time analysis results further revealed that each cluster was distributed in different positions along the path and that a bifurcation

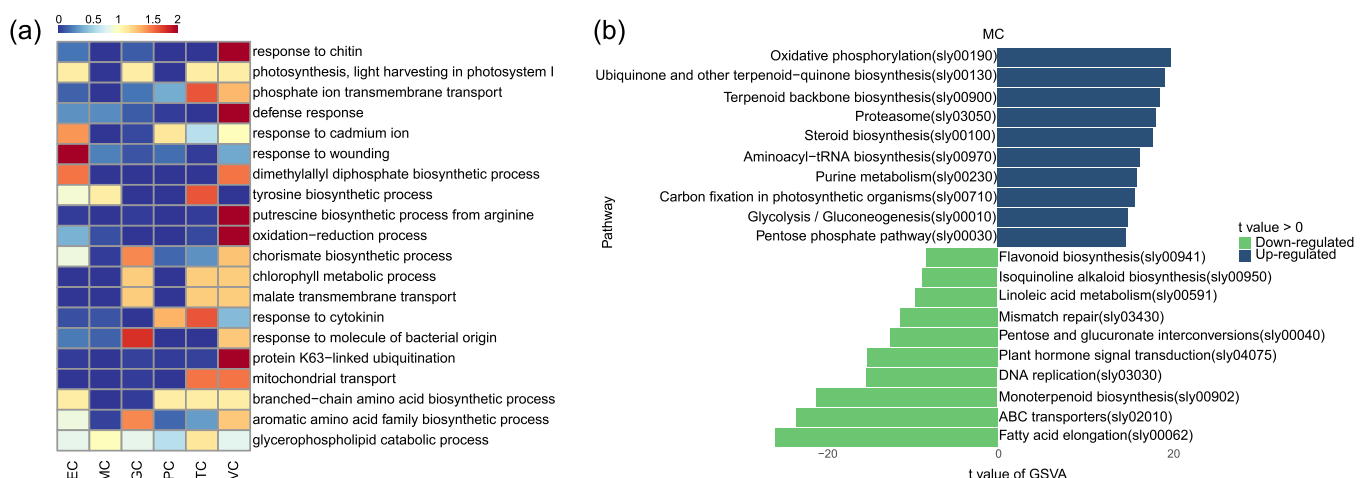


FIGURE 4 Tomato chlorosis virus (ToCV) infection of each cell type. (a) GO pathway enrichment analysis of each cell type in ToCV-infected tomato leaf. (b) GSVA analysis of DEGs affected by ToCV-infection in the mesophyll cell (MC). GSVA, gene set variation analyses. [Color figure can be viewed at wileyonlinelibrary.com]

point marked the developmental state's transition, and the pseudotime trajectory had two branch points that divided all cells into five states (Figure 5b). Based on the pseudotime value of each mesophyll cell, we screened the DGEs along the pseudotime line and performed cluster analysis. The DGEs were grouped into four modules by similarity in expression trends. These genes were divided into four modules that showed different gene expression patterns, reflecting transcriptional rewiring during the development of mesophyll cells

infected with ToCV (Figure 5c). The gene expression in modules 1 and 3 increased at the end of the pseudotime axis (Figure 5c). In contrast, gene expression gradually decreased with pseudotime in module 4, while module 2 showed an increasing trend followed by a decrease (Figure 5c).

In combination with GO function analysis, the results showed that most defence-related genes showed a trend of significantly upregulated expression with increasing proposed time (Figure 5c).

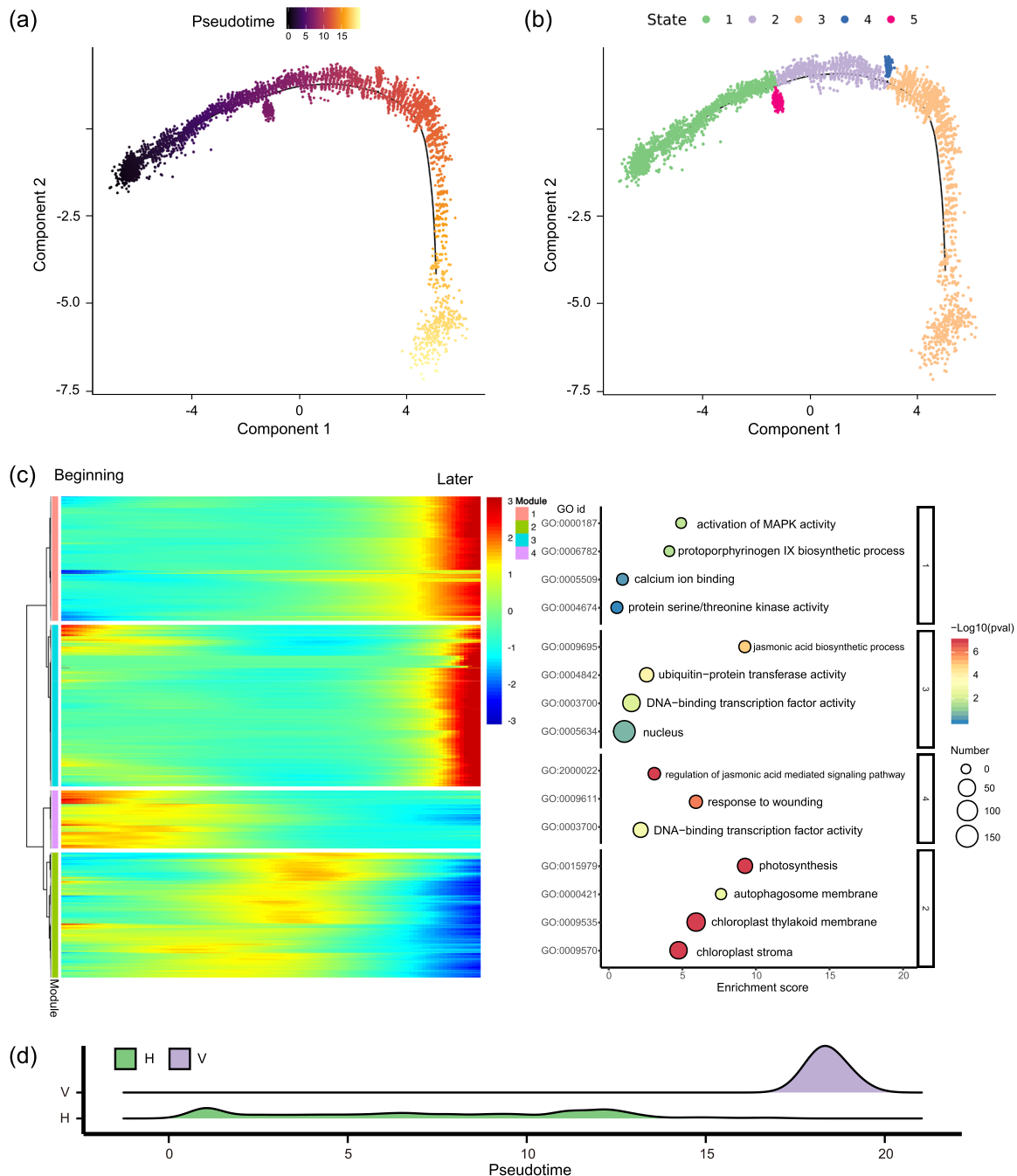


FIGURE 5 Differentiation trajectory of trichome cells. (a, b) Distribution of cells in each cluster on the pseudo-time trajectory. (c) Heatmap showing expression of the most significant DEGs in three modules across the pseudo-time. Representative GO terms for each module are shown on the right. (d) Pseudo-time ridge map. The X-axis shows time from morning to night from left to right, and the Y-axis shows different samples. DEGs, differentially expressed genes. [Color figure can be viewed at wileyonlinelibrary.com]

This is consistent with the trend of expression in ToCV-infected cells over time (Figure 5d). Additionally, genes in module 4 were most enriched in regulation of jasmonic acid-mediated signalling pathway, and this suggests that jasmonic acid may play a key role in the early stages of ToCV-infected mesophyll cells (Figure 5c). In conclusion, the pseudo-time analysis provided insight into the dynamics of tomato leaf cell-type development under biotic stress, which suggests that ToCV infection causes mesophyll cells to differentiate in a way that enhances the plant's defences (Table S7).

3.6 | Identification of the core transcriptional factors regulating the response to ToCV in tomato leaves

The development of the plant is under the control of a complex transcription regulatory network. To identify the master regulators related to the biogenesis and development of cells of tomato leaves, we screened for TFs that are specifically expressed in epidermal cells, guard cells, mesophyll cells, proliferating cells, trichome cells and vascular cells. TF-target gene regulatory networks for these cell clusters were then generated, and the core TFs were identified (Table S8). As is shown in Figure 6a, TFs solyc10g006130.1, solyc03g093550.1 and solyc04g077980.1 play specific regulations in epidermal cells, mesophyll cells and vascular cells, respectively. From the analysis, we can clearly see that the core TF solyc10g009110.1 (ERF4) plays a central regulatory role in all cell types. Notably, ERF4 has a large number of edges, indicating that it has the most targeted regulatory genes. Therefore, ERF4 may play a key role in ToCV-infected tomato cells. From the regulatory network of TFs (Figure 6a; Figure S8), we found that ERF4 targeted the F-box protein SKIP2, and this gene was upregulated after ToCV infection (Table S6). F-box proteins are substrate-recognition components of Skp1-Rbx1-Cul1-F-box protein ubiquitin ligases (Xu et al., 2009), and ubiquitinated E3 ligases involved in plant growth and developmental processes, such as photomorphogenesis and abiotic stress (Mendiondo et al., 2016; Ling et al., 2021; Al-Saharin et al., 2022). Therefore, we performed a yeast one-hybrid assay to determine whether ERF4 could regulate SSKIP2 expression. The results showed that ERF4 could bind the promoter of SSKIP2 to drive the expression of the reporter and support yeast growth on a minimal medium (Figure 6b). A dual luciferase assay confirmed the ability of ERF4 to bind the SSKIP2 promoter and drive luciferase expression (Figure 6c).

3.7 | Subcellular localization and functional analysis of the SSKIP2

To clarify the location of its expression, we generate the SSKIP2-eGFP fusion genes driven by a CaMV35S promoter. Upon co-expression of SSKIP2 and the red nuclear marker RFP-H2b in *Nicotiana benthamiana* leaves. The overlay of the GFP fluorescence with the red signal revealed that the SSKIP2 fusion protein was

localized to the cytomembrane but also to the nucleus (Figure 6d). A typical symptom of ToCV infection in tomatoes is leaf yellowing. SSKIP2 knockout tomato showed a better leaf green state before and after ToCV infection than the control (Figure 6e). Similarly, the chlorophyll content was higher in the mutant tomato (Figure 6f). In conclusion, our results reveal that ERF4 regulates SSKIP2, and the latter plays a crucial role in chlorophyll maintenance during ToCV infection in tomato leaves.

4 | DISCUSSION

The development of single-cell sequencing technology has provided possibilities for exploring plant growth and development at the single-cell level (Rich-Griffin et al., 2020; Shaw et al., 2021). Protoplasts were successfully isolated from healthy and ToCV-infected tomato leaves, and tomato leaf cell atlas was constructed successfully using scRNA-Seq technology and used to elucidate the response of tomato leaves to virus infection (Figure 1). We believe our results will provide a reference for future applications of single-cell technology to other non-model plants and for studying plant leaf cell function under biotic stress.

As few tomato cell marker genes exist, various strategies have been used to identify tomato leaf cell types. Previous single-cell studies on rice seedlings have confirmed that various marker genes may not be conserved in different plants. Therefore, it is not suitable for reliable cell identification across species (Liu et al., 2021a). To identify cell types in tomato leaves, in addition to the combination of a small number of known marker genes and GO functions, MIA was applied (Figure 1d; Figure S2 and Table S3). Our identification method provides a reference for other plant single-cell studies with fewer known marker genes. In addition, to identify potential tomato leaf cell marker genes, we characterized the highly expressed genes in each cell cluster (Figure 2a,b). Moreover, we verified the expression of potential marker genes in different cell types by *in situ* hybridization (Figure 2c–e). We confirmed that the identified marker genes could be used for subsequent tomato cell type identification.

Applying scRNA-seq in the study of plant responses to viral stress can help reveal the main cell clusters and genes involved in immune resistance pathways (Liu et al., 2021b). By comparing cells from leaves grown under ToCV infection, we discovered that ToCV does not substantially alter cell type identity but leads to changes in the relative proportions of cell types. We can clearly notice that the proportion of cell types changed significantly after ToCV infection (Figure 3a,b). Moreover, the transcriptional characteristics vary among different cell types, and more specific DEGs can be observed in vascular cells, guard cells, and mesophyll cells (Figure 3c; Figure S5b). Chlorophyll is mainly present in mesophyll cells, which is the main reason for the green appearance of leaves and is directly related to plant photosynthesis (Borsuk and Brodersen, 2019). This is consistent with our results, as we found that ToCV infection leads to tomato leaf yellowing and chlorophyll reduction while also

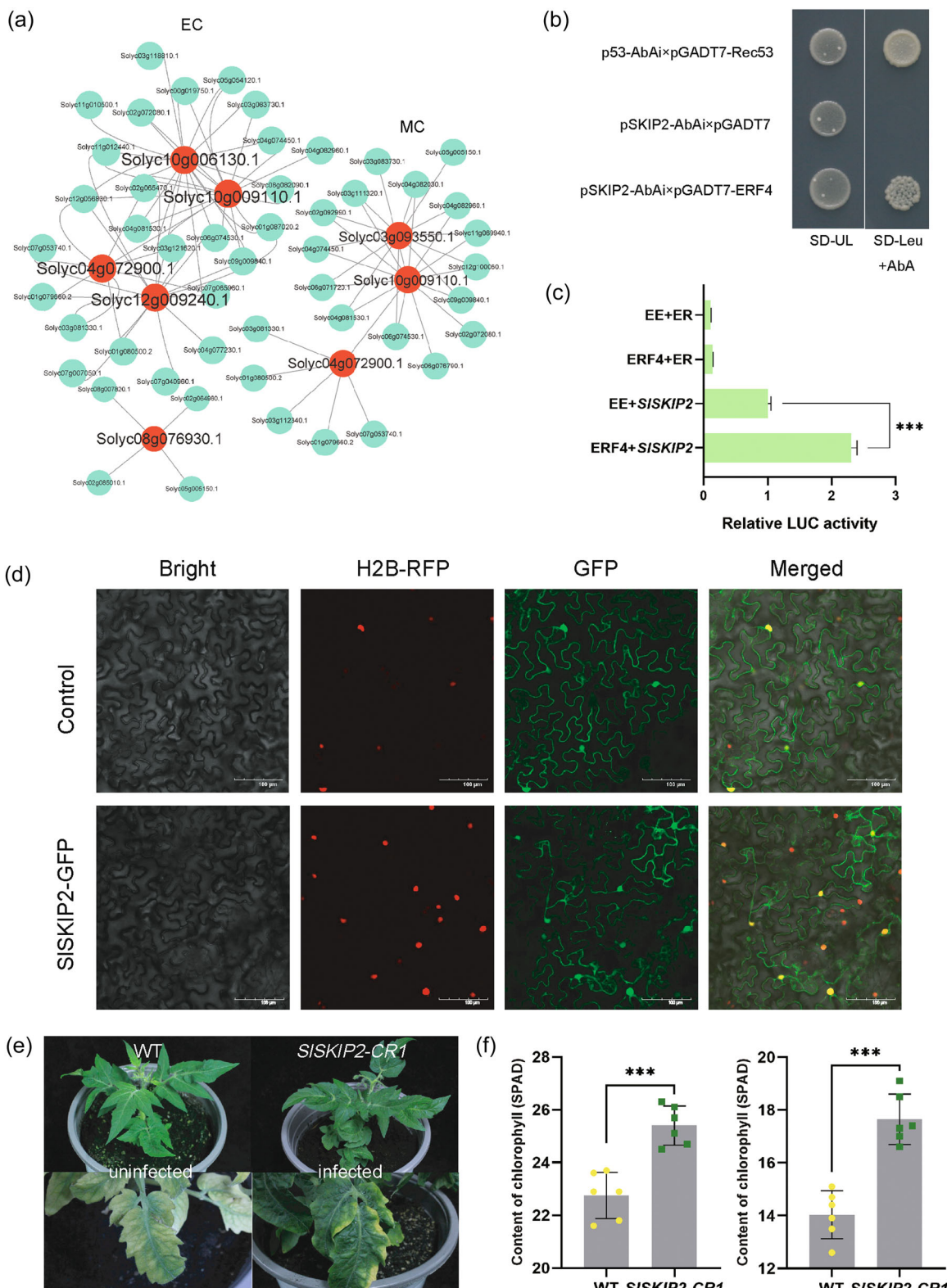


FIGURE 6 Construction of regulatory networks of transcription factors in different cell types. (a) The regulatory network of TFs identified in cell types of tomato chlorosis virus (ToCV)-infected tomato leaf. EC, epidermal cells. MC, mesophyll cells. (b) Yeast-one-hybrid analysis of ERF4 binding to the promoter region of *SISKIP2*. Interaction was determined on selective dropout (SD)/-Leu medium in the presence of aureobasidin A (AbA). (c) Dual-LUC assays showing the interaction between ERF4 and the *SISKIP2* promoter. (d) Subcellular localization of *SISKIP2*-GFP in *Nicotiana benthamiana*. The pFGC-GFP alone was used as control. GFP, green fluorescent protein fluorescence; H2b-RFP, red fluorescent protein fluorescence of nucleic marker; Merge, merged image of GFP, H2b-RFP and bright field signals. (e) Plant phenotype of control tomato and knockout tomato with ToCV infection or without ToCV infection. (f) Chlorophyll content of control tomato and transgenic tomato with ToCV infection or without ToCV infection. Values are means \pm SE. Asterisks denote significant differences ($p < 0.05$). TFs, transcription factors. [Color figure can be viewed at wileyonlinelibrary.com]

causing damage to the internal structure of the leaves (Figure 3d-f). Moreover, the upregulated DEGs were enriched in 'chlorophyll metabolic process' in epidermal cells, mesophyll cells and proliferating cells. Significant variation in the number of specific cell types implied a complex response manner in tomato leaves infected with ToCV. Combined with the GO annotations, we know that the defence-related genes of guard cells infected with ToCV were significantly upregulated (Figure 4a; Table S6). Stomata, composed of guard cells, play a central role in plant growth, especially in response to abiotic and biotic stresses (Melotto et al., 2008; Assmann and Jegla, 2016; Lin et al., 2022). A previous study in *Arabidopsis* roots found that gene expression differences were primarily tissue- or cell-type-specific, with 49% of the DEGs altered in a single tissue or cell type and only 1% altered throughout the root (Shulse et al., 2019). Additionally, it has been demonstrated that the response of rice seedlings to abiotic stress works in a cell-specific manner (Wang et al., 2021). Our results showed the cell types of tomato leaves response to ToCV infection in a specific manner (Figure S5b). However, enrichment analysis showed that biological processes were shared among the ToCV-infected cell types, such as the GO terms 'response to chitin' and 'response to wounding' (Figure 4a).

Secondary metabolites play an essential biological role in mediating plant responses to biotic and abiotic stressors (Mishra et al., 2020). A previous study showed that the concentration of flavonols and hydroxycinnamic acids increased following infection with grapevine leafroll-associated virus 3 (Montero et al., 2016). Our findings also suggested that secondary metabolite synthesis and metabolic pathways were enriched significantly in ToCV-infected cell types (Figure 4b; Figure S7). Plant terpenoids are derived from five-carbon isoprene units, which act as chemically interacting molecules and protect plants from nonbiological and biological environmental conditions (Yang et al., 2012). Pathogen infection induces the release of plant-related volatiles, which usually attract the natural enemies of herbivores or avoid insects (Aljbory and Chen, 2018; Sharifi et al., 2018). For example, *cucumber mosaic virus* effector protein 2b increases the migration of green peach aphids to infect *Arabidopsis* plants. However, it reduces their sedimentation in virus-infected plants (Wu et al., 2017). ToCV infection significantly enriched in terpenoid backbone synthesis in mesophyll cell (Figure 4b). Plant volatiles mediate whitefly preference for virus transmission (Sharifi et al., 2018), which may be one of the reasons for the rapid spread of ToCV. Moreover, ToCV-infected cell types exhibited significantly upregulated gene sets involved in the MAPK signalling pathway-plant and plant-pathogen interactions (Table S6). At the same time, the MAPK cascade is a highly conserved signalling module that plays a crucial role in the defence response against pathogens (Miya et al., 2007; Yin et al., 2021). Pathogens can inhibit the BR pathway of plants to facilitate viral infection (Mei et al., 2018; Mei et al., 2021). We found that the steroid biosynthesis pathway was induced significantly in the ToCV-infected cells. This indicates that ToCV may be able to infect plants through complex interactions with the steroid pathway.

The mesophyll cells' differentiation trajectory and gene expression were characterized after ToCV infection (Figure 5). When viruses attack plants, relevant defence responses are implemented to ensure their survival (Nobori and Tsuda, 2019). Therefore, we speculated that the cells tend to differentiate in a direction beneficial to plant growth; thus, we attempted to use a pseudo-time analysis to verify this hypothesis. At the start of the pseudo-time axis, GO analysis showed that genes with high expression were enriched in 'regulation of jasmonic acid mediated signalling pathway' (Figure 5c; Table S7). This is consistent with previous studies, where jasmonic acid played a positive role in the early defence response (Jarad et al., 2020). Not surprisingly, at the end of the differentiation trajectory, the genes in the ToCV-infected mesophyll cells were the most abundant in defence-related terms (Figure 5c; Table S7). Furthermore, in Module 2, the differential genes were mainly enriched in chloroplast and photosynthesis-related pathways, suggesting complex interactions with leaf chloroplasts during ToCV infection (Figure 5c; Table S7). Gene expression analysis of the cell differentiation process is likely to help us identify the valuable genes. Combined with ToCV-induced plant phenotypes, it is not difficult to speculate that these genes may play a key role in the defence of leaf chloroplasts against ToCV infection, although this requires further experimental verification.

TFs have been widely studied as critical regulators of plant immune responses to various biological stressors (Wani et al., 2021). For example, OsWRKY62 was reported to be a negative regulator of the innate defence response against bacterial blight in rice, whereas OsWRKY67 acts as a positive regulator of PTI and ETI against two rice pathogens (Vo et al., 2018). The WRKY family gene WRKY75 (FvH4_4g23480) is overexpressed in each cell type of early *Botrytis cinerea*-infected woodland strawberry (Bai et al., 2022). In our data, the WRKY TFs were the most highly expressed TF detected, demonstrating different degrees of differential expression in each cell type (Table S6). This suggests that WRKY TFs may play an essential role in the interaction between ToCV and plants, consistent with previous studies (Yue et al., 2021). In addition, TF families, such as basic helix-loop-helix (BHLH), APETALA2/ethylene-responsive factor and zinc finger protein, were also expressed in large amounts in ToCV-infected cells. The critical role of these genes in the plant response to stress has been reported (Table S6) (Qian et al., 2021; Ritonga et al., 2021). Moreover, regulatory network analysis suggested that ERF4 may play a vital role as a core TF in tomato response to ToCV (Figure 6a; Figure S8). With reduced HvPRT6 expression, transgenic plants exhibit sustained biomass, increased yield, and chlorophyll retention under waterlogging (Mendiondo et al., 2016). Inhibition of PUB22/PUB23 results in *Arabidopsis* insensitivity to sodium arsenite and the maintenance of green cotyledons during seed germination (Ahn et al., 2022). The chlorophyll content is an indispensable pigment for absorbing light energy and transferring electrons during photosynthesis (Hu et al., 2021); our results demonstrated that ERF4 regulates SISKIP2, and the latter plays a crucial role in chlorophyll maintenance during ToCV infection in tomato leaves (Figure 6b-f).

The emergence and continuous development of single-cell sequencing technology is a powerful tool for us to study the process of plant growth at the cellular level (Rich-Griffin et al., 2020). However, there are still some limitations. For example, the preparation of protoplasts cannot form a general method, especially when it comes to plant research in stress, which will lead to the prepared protoplasts very fragile and the activity fluctuates greatly. Moreover, some species have few known marker genes and cannot accurately identify cell types, such as some species with little research and even have no reference genome. However, the application of mononuclear and spatial transcriptomics in plants in recent years has solved the short board of single-cell sequencing to a certain extent (Liu et al., 2021b). We believe that the unpredictable development of technology and the combined application of multiomics in the future will bring us unlimited possibilities to study the mechanism of plant development.

5 | CONCLUSION

In summary, we successfully applied single-cell sequencing to tomato leaves, allowing us to construct a cell map of the tomato leaf. Our results showed that the tomato leaves were composed of highly heterogeneous cells. The potential marker genes of tomato leaves characterized in this study can be a subsequent single-cell plant research. Comparisons of leaf cells with or without viral infection indicated that ToCV infection-induced transcriptomic changes vary among cell types. Furthermore, the reduction in the number of mesophyll cells is positively correlated with the pathologic changes. We also demonstrated that *SISKP2* is essential for chlorophyll maintenance in ToCV-infected tomato leaves, and it had a direct interaction with ERF4. Together, our results provide a valuable resource for studying the developmental and physiological functions of plant cell types under biological stress at the molecular level and single-cell resolution.

ACKNOWLEDGEMENTS

This work was supported by the National Natural Science Foundation of Hunan Province (No. 2023JJ10026), the National Natural Science Foundation of China (Nos. 32030088, 32072383, 32272535, 31901854), and the Agriculture Research System of China (No. CARS-23-D-02).

CONFLICT OF INTEREST STATEMENT

The authors declare no conflicts of interest.

DATA AVAILABILITY STATEMENT

The raw data of single RNA-seq have been deposited in the NCBI GEO with the accession number GSE201931.

ORCID

Hao Yue  <http://orcid.org/0000-0001-9645-6181>

Ted C. J. Turlings  <http://orcid.org/0000-0002-8315-785X>

REFERENCES

- Ahn, M.Y., Seo, D.H. & Kim, W.T. (2022) PUB22 and PUB23 u-box E3 ubiquitin ligases negatively regulate 26S proteasome activity under proteotoxic stress conditions. *Journal of Integrative Plant Biology*, 64, 625–631.
- Aljbory, Z. & Chen, M.S. (2018) Indirect plant defense against insect herbivores: a review. *Insect Science*, 25, 2–23.
- Al-Saharin, R., Hellmann, H. & Mooney, S. (2022) Plant E3 ligases and their role in abiotic stress response. *Cells*, 11, 890.
- Assmann, S.M. & Jegla, T. (2016) Guard cell sensory systems: recent insights on stomatal responses to light, abscisic acid, and CO₂. *Current Opinion in Plant Biology*, 33, 157–167.
- Bai, Y., Liu, H., Lyu, H., Su, L., Xiong, J. & Cheng, Z.M. (2022) Development of a single-cell atlas for woodland strawberry (*Fragaria vesca*) leaves during early *Botrytis cinerea* infection using single-cell RNA-seq. *Horticulture Research*, 9, uhab055.
- Bonke, M., Thitamadee, S., Mähönen, A.P., Hauser, M.T. & Helariutta, Y. (2003) APL regulates vascular tissue identity in. *Nature*, 426, 181–186.
- Borsuk, A.M. & Brodersen, C.R. (2019) The spatial distribution of chlorophyll in leaves. *Plant Physiology*, 180, 1406–1417.
- Butler, A., Hoffman, P., Smibert, P., Papalexi, E. & Satija, R. (2018) Integrating single-cell transcriptomic data across different conditions, technologies, and species. *Nature Biotechnology*, 36, 411–420.
- Chen, L., Yang, D., Zhang, Y., Wu, L., Zhang, Y., Ye, L. et al. (2018) Evidence for a specific and critical role of mitogen-activated protein kinase 20 in uni-to-binucleate transition of microgametogenesis in tomato. *New Phytologist*, 219, 176–194.
- Denyer, T., Ma, X., Klesen, S., Scacchi, E., Nieselt, K. & Timmermans, M.C.P. (2019) Spatiotemporal developmental trajectories in the *Arabidopsis* root revealed using high-throughput single-cell RNA sequencing. *Developmental Cell*, 48, 840–852.e5.
- Du, F., Guan, C. & Jiao, Y. (2018) Molecular mechanisms of leaf morphogenesis. *Molecular Plant*, 11(9), 1117–1134.
- Efroni, I. & Birnbaum, K.D. (2016) The potential of single-cell profiling in plants. *Genome Biology*, 17, 65.
- Endo, M., Shimizu, H., Nohales, M.A., Araki, T. & Kay, S.A. (2014) Tissue-specific clocks in *Arabidopsis* show asymmetric coupling. *Nature*, 515, 419–422.
- Fortes, I.M. & Navas-Castillo, J. (2012) Potato, an experimental and natural host of the crinivirus tomato chlorosis virus. *European Journal of Plant Pathology*, 134, 81–86.
- Gessain, A. & García-Arenal, F. (2015) Editorial overview: emerging viruses: interspecies transmission. *Current Opinion in Virology*, 10, v–viii.
- Hu, X., Gu, T., Khan, I., Zada, A. & Jia, T. (2021) Research progress in the interconversion, turnover and degradation of chlorophyll. *Cells*, 10, 3134.
- Jarad, M., Mariappan, K., Almeida-Trapp, M., Mette, M.F., Mithöfer, A., Rayapuram, N. et al. (2020) The lamin-like LITTLE NUCLEI 1 (LINC1) regulates pattern-triggered immunity and jasmonic acid signaling. *Frontiers in Plant Science*, 10, 1639.
- Javelle, M., Vernoud, V., Rogowsky, P.M. & Ingram, G.C. (2011) Epidermis: the formation and functions of a fundamental plant tissue. *New Phytologist*, 189, 17–39.
- Jean-Baptiste, K., McFafine-Figueroa, J.L., Alexandre, C.M., Dorrrity, M.W., Saunders, L., Bubb, K.L. et al. (2019) Dynamics of gene expression in single root cells of *Arabidopsis thaliana*. *The Plant Cell*, 31, 993–1011.
- Kim, J.Y., Symeonidi, E., Pang, T.Y., Denyer, T., Weidauer, D., Bezrutczyk, M. et al. (2021) Distinct identities of leaf phloem cells revealed by single cell transcriptomics. *The Plant Cell*, 33, 511–530.
- Lex, A., Gehlenborg, N., Strobelt, H., Vuillemot, R. & Pfister, H. (2014) UpSet: visualization of intersecting sets. *IEEE transactions on visualization and computer graphics*, 20, 1983–1992.

- Liang, X., Ma, Z., Ke, Y., Wang, J., Wang, L., Qin, B. et al. (2023) Single-cell transcriptomic analyses reveal cellular and molecular patterns of rubber tree response to early powdery mildew infection. *Plant, Cell & Environment*, 46, 2222–2237.
- Libault, M., Pingault, L., Zogli, P. & Schiefelbein, J. (2017) Plant systems biology at the single-cell level. *Trends in Plant Science*, 22, 949–960.
- Lin, P.A., Chen, Y., Ponce, G., Acevedo, F.E., Lynch, J.P., Anderson, C.T. et al. (2022) Stomata-mediated interactions between plants, herbivores, and the environment. *Trends in Plant Science*, 27, 287–300.
- Ling, Q., Sadali, N.M., Soufi, Z., Zhou, Y., Huang, B., Zeng, Y. et al. (2021) The chloroplast-associated protein degradation pathway controls chromoplast development and fruit ripening in tomato. *Nature Plants*, 7, 655–666.
- Liu, H., Hu, D., Du, P., Wang, L., Liang, X. & Li, H. et al. (2021b) Single-cell RNA-seq describes the transcriptome landscape and identifies critical transcription factors in the leaf blade of the allotetraploid peanut (*Arachis hypogaea* L.). *Plant Biotechnology Journal*, 19, 2261–2276.
- Liu, Q., Liang, Z., Feng, D., Jiang, S., Wang, Y., Du, Z. et al. (2021a) Transcriptional landscape of rice roots at the single-cell resolution. *Molecular Plant*, 14, 384–394.
- Lozano, G., Moriones, E. & Navas-Castillo, J. (2006) Complete nucleotide sequence of the RNA2 of the crinivirus tomato chlorosis virus. *Archives of Virology*, 151, 581–587.
- Ma, X., Zhang, Q., Zhu, Q., Liu, W., Chen, Y., Qiu, R. et al. (2015) A robust CRISPR/Cas9 system for convenient, high-efficiency multiplex genome editing in monocot and dicot plants. *Molecular Plant*, 8, 1274–1284.
- Macosko, E.Z., Basu, A., Satija, R., Nemesh, J., Shekhar, K., Goldman, M. et al. (2015) Highly parallel genome-wide expression profiling of individual cells using nanoliter droplets. *Cell*, 161, 1202–1214.
- Mei, Y., Wang, Y., Hu, T., He, Z. & Zhou, X. (2021) The C4 protein encoded by tomato leaf curl Yunnan virus interferes with mitogen-activated protein kinase cascade-related defense responses through inhibiting the dissociation of the ERECTA/BKI1 complex. *New Phytologist*, 231, 747–762.
- Mei, Y., Yang, X., Huang, C., Zhang, X. & Zhou, X. (2018) Tomato leaf curl Yunnan virus-encoded C4 induces cell division through enhancing stability of Cyclin D 1.1 via impairing NbSKn⁻mediated phosphorylation in *Nicotiana benthamiana*. *PLoS Pathogens*, 14, e1006789.
- Melotto, M., Underwood, W. & He, S.Y. (2008) Role of stomata in plant innate immunity and foliar bacterial diseases. *Annual Review of Phytopathology*, 46, 101–122.
- Mendiondo, G.M., Gibbs, D.J., Szurman-Zubrzycka, M., Korn, A., Marquez, J., Szarejko, I. et al. (2016) Enhanced waterlogging tolerance in barley by manipulation of expression of the N-end rule pathway E3 ligase PROTEOLYSIS6. *Plant Biotechnology Journal*, 14, 40–50.
- Mishra, J., Srivastava, R., Trivedi, P.K. & Verma, P.C. (2020) Effect of virus infection on the secondary metabolite production and phytohormone biosynthesis in plants. *3 Biotech*, 10, 547.
- Miya, A., Albert, P., Shinya, T., Desaki, Y., Ichimura, K., Shirasu, K. et al. (2007) CERK1, a LysM receptor kinase, is essential for chitin elicitor signaling in *Arabidopsis*. *Proceedings of the National Academy of Sciences*, 104, 19613–19618.
- Moncada, R., Barkley, D., Wagner, F., Chiodin, M., Devlin, J.C., Baron, M. et al. (2020) Integrating microarray-based spatial transcriptomics and single-cell RNA-seq reveals tissue architecture in pancreatic ductal adenocarcinomas. *Nature Biotechnology*, 38, 333–342.
- Montero, R., Pérez-Bueno, M.L., Barón, M., Florez-Sarasa, I., Tohge, T., Fernie, A.R. et al. (2016) Alterations in primary and secondary metabolism in *Vitis vinifera* "Malvasía de Banyalbufar" upon infection with Grapevine leafroll-associated virus 3. *Physiologia Plantarum*, 157, 442–452.
- Nobori, T. & Tsuda, K. (2019) The plant immune system in heterogeneous environments. *Current Opinion in Plant Biology*, 50, 58–66.
- Ortiz-Ramírez, C., Guillotin, B., Xu, X., Rahni, R., Zhang, S., Yan, Z. et al. (2021) Ground tissue circuitry regulates organ complexity in maize and *Setaria*. *Science*, 374, 1247–1252.
- Pallás, V., Sánchez-Navarro, J.A. & James, D. (2018) Recent advances on the multiplex molecular detection of plant viruses and viroids. *Frontiers in Microbiology*, 9, 2087.
- Qian, Y., Zhang, T., Yu, Y., Gou, L., Yang, J., Xu, J. et al. (2021) Regulatory mechanisms of bHLH transcription factors in plant adaptive responses to various abiotic stresses. *Frontiers in Plant Science*, 12, 677611.
- Rich-Griffin, C., Stechemesser, A., Finch, J., Lucas, E., Ott, S. & Schäfer, P. (2020) Single-cell transcriptomics: a high-resolution avenue for plant functional genomics. *Trends in Plant Science*, 25, 186–197.
- Ritchie, M.E., Phipson, B., Wu, D., Hu, Y., Law, C.W., Shi, W. et al. (2015) Limma powers differential expression analyses for RNA-sequencing and microarray studies. *Nucleic Acids Research*, 43, e47.
- Ritonga, F.N., Ngatia, J.N., Wang, Y., Khoso, M.A., Farooq, U. & Chen, S. (2021) AP2/ERF, an important cold stress-related transcription factor family in plants: a review. *Physiology and Molecular Biology of Plants*, 27, 1953–1968.
- Ruonala, R., Ko, D. & Helariutta, Y. (2017) Genetic networks in plant vascular development. *Annual Review of Genetics*, 51, 335–359.
- Sawchuk, M.G., Donner, T.J., Head, P. & Scarpella, E. (2008) Unique and overlapping expression patterns among members of photosynthesis-associated nuclear gene families in *Arabidopsis*. *Plant Physiology*, 148, 1908–1924.
- Sharifi, R., Lee, S.M. & Ryu, C.M. (2018) Microbe-induced plant volatiles. *New Phytologist*, 220, 684–691.
- Shaw, R., Tian, X. & Xu, J. (2021) Single-cell transcriptome analysis in plants: advances and challenges. *Molecular Plant*, 14, 115–126.
- Shi, X., Zhang, Z., Zhang, C., Zhou, X., Zhang, D. & Liu, Y. (2021) The molecular mechanism of efficient transmission of plant viruses in variable virus–vector–plant interactions. *Horticultural Plant Journal*, 7, 501–508.
- Shulse, C.N., Cole, B.J., Ciobanu, D., Lin, J., Yoshinaga, Y., Gouran, M. et al. (2019) High-throughput single-cell transcriptome profiling of plant cell types. *Cell Reports*, 27, 2241–2247.e4.
- Sun, H., Zhang, H., Xu, Z., Wang, Y., Liu, X., Li, Y. et al. (2021) TMT-based quantitative proteomic analysis of the effects of *pseudomonas syringae* pv. *tabaci* (Pst) infection on photosynthetic function and the response of the MAPK signaling pathway in tobacco leaves. *Plant Physiology and Biochemistry*, 166, 657–667.
- Sun, X., Feng, D., Liu, M., Qin, R., Li, Y., Lu, Y. et al. (2022) Single-cell transcriptome reveals dominant subgenome expression and transcriptional response to heat stress in Chinese cabbage. *Genome Biology*, 23, 262.
- Takada, S., Takada, N. & Yoshida, A. (2013) ATML1 promotes epidermal cell differentiation in *Arabidopsis* shoots. *Development*, 140, 1919–1923.
- Trapnell, C., Cacchiarelli, D., Grimsby, J., Pokharel, P., Li, S., Morse, M. et al. (2014) The dynamics and regulators of cell fate decisions are revealed by pseudotemporal ordering of single cells. *Nature Biotechnology*, 32, 381–386.
- Velasco, L., Simón, B., Janssen, D. & Cenis, J.I. (2008) Incidences and progression of tomato chlorosis virus disease and tomato yellow leaf curl virus disease in tomato under different greenhouse covers in southeast Spain. *Annals of Applied Biology*, 153, 335–344.
- Vo, K.T.X., Kim, C.Y., Hoang, T.V., Lee, S.K., Shirsekar, G., Seo, Y.S. et al. (2018) OsWRKY67 plays a positive role in basal and XA21-mediated resistance in rice. *Frontiers in Plant Science*, 8, 2220.
- Wang, Y., Huan, Q., Li, K. & Qian, W. (2021) Single-cell transcriptome atlas of the leaf and root of rice seedlings. *Journal of Genetics and Genomics*, 48, 881–898.

- Wani, S.H., Anand, S., Singh, B., Bohra, A. & Joshi, R. (2021) WRKY transcription factors and plant defense responses: latest discoveries and future prospects. *Plant Cell Reports*, 40, 1071–1085.
- Wendrich, J.R., Yang, B., Vandamme, N., Verstaen, K., Smet, W., Van de Velde, C. et al. (2020) Vascular transcription factors guide plant epidermal responses to limiting phosphate conditions. *Science*, 370, eaay4970.
- Wisler, G.C., Duffus, J.E., Liu, H.Y. & Li, R.H. (1998a) Ecology and epidemiology of Whitefly-Transmitted closteroviruses. *Plant Disease*, 82, 270–280.
- Wisler, G.C., Li, R.H., Liu, H.Y., Lowry, D.S. & Duffus, J.E. (1998b) Tomato chlorosis virus: a new whitefly-transmitted, phloem-limited, bipartite closterovirus of tomato. *Phytopathology*, 88, 402–409.
- Wu, D., Qi, T., Li, W.X., Tian, H., Gao, H., Wang, J. et al. (2017) Viral effector protein manipulates host hormone signaling to attract insect vectors. *Cell Research*, 27, 402–415.
- Xu, G., Ma, H., Nei, M. & Kong, H. (2009) Evolution of F-box genes in plants: different modes of sequence divergence and their relationships with functional diversification. *Proceedings of the National Academy of Sciences*, 106, 835–840.
- Yang, C.Q., Fang, X., Wu, X.M., Mao, Y.B., Wang, L.J. & Chen, X.Y. (2012) Transcriptional regulation of plant secondary metabolism ^F. *Journal of Integrative Plant Biology*, 54, 703–712.
- Yang, H., Zu, G., Liu, Y., Xie, D., Gan, X. & Song, B. (2020) Tomato chlorosis virus minor coat protein as a novel target to screen antiviral drugs. *Journal of Agricultural and Food Chemistry*, 68, 3425–3433.
- Yin, Z., Zhu, W., Zhang, X., Chen, X., Wang, W., Lin, H. et al. (2021) Molecular characterization, expression and interaction of MAPK, MAPKK and MAPKKK genes in upland cotton. *Genomics*, 113, 1071–1086.
- Yue, H., Huang, L.P., Lu, D.Y.H., Zhang, Z.H., Zhang, Z., Zhang, D.Y. et al. (2021) Integrated analysis of microRNA and mRNA transcriptome reveals the molecular mechanism of *Solanum lycopersicum* response to *Bemisia tabaci* and tomato chlorosis virus. *Frontiers in Microbiology*, 12, 693574.
- Zhang, T.Q., Chen, Y. & Wang, J.W. (2021) A single-cell analysis of the *Arabidopsis* vegetative shoot apex. *Developmental Cell*, 56, 1056–1074.e8.
- Zhang, T.Q., Lian, H., Zhou, C.M., Xu, L., Jiao, Y. & Wang, J.W. (2017) A two-step model for de novo activation of WUSCHEL during plant shoot regeneration. *The Plant Cell*, 29, 1073–1087.
- Zhang, T.Q., Xu, Z.G., Shang, G.D. & Wang, J.W. (2019) A single-cell RNA sequencing profiles the developmental landscape of *Arabidopsis* root. *Molecular Plant*, 12, 648–660.
- Zhong, X., Yu, X. & Chang, H. (2022) Exploration of a novel prognostic nomogram and diagnostic biomarkers based on the activity variations of hallmark gene sets in hepatocellular carcinoma. *Frontiers in Oncology*, 12, 830362.

SUPPORTING INFORMATION

Additional supporting information can be found online in the Supporting Information section at the end of this article.

How to cite this article: Yue, H., Chen, G., Zhang, Z., Guo, Z., Zhang, Z., Zhang, S. et al. (2024) Single-cell transcriptome landscape elucidates the cellular and developmental responses to tomato chlorosis virus infection in tomato leaf. *Plant, Cell & Environment*, 47, 2658–2672.

<https://doi.org/10.1111/pce.14906>